

Alessandro Dosio *, **Jordi Vilà-Guerau de Arellano**, **Albert A.M. Holtslag**,
Meteorology and Air Quality Group, Wageningen University, Wageningen, The Netherlands
Peter J.H. Bultjes
TNO-MEP, Apeldoorn, The Netherlands

1. INTRODUCTION

Dispersion of a passive scalar in the Convective Boundary Layer (CBL) is driven by buoyancy and wind shear. The latter contributes to the enhancement of the horizontal plume's spread (Venkatram, 1988). Although dispersion in a pure convective boundary layer (no shear effect considered) is a process that has been largely investigated over the last few decades, only a few studies have analyzed directly the effect of wind shear on plume dispersion (Mason, 1993; Luhar, 2002). Moreover many parameterizations used in applied dispersion models do not consider shear contributions at short distances, except under very stable conditions (Gryning et al, 1986).

This study is therefore meant to investigate the dispersion of a line source of inert tracer in a buoyancy and shear-driven boundary layer by means of a Large Eddy Simulation (LES) numerical model, following the approach of Nieuwstadt and De Valk (1987). Different combinations of buoyancy force (surface heat flux) and geostrophic wind are used to generate boundary layers that are classified according to stability parameters ($-z_i/L$, u_*/w_* where z_i is the CBL height, L is the Monin-Obukhov length u_* is the friction velocity and w_* the convective scaling velocity).

Model results for the pure convective cases are first compared with different data set (numerical and laboratory studies) to evaluate the model's performances. By using a similar numerical setup, the effect of wind shear on the horizontal dispersion in different shear-driven boundary layers is then studied.

We finally discuss the parameterization proposed by Luhar (2002) which takes into account the shear contribution to the horizontal dispersion parameter (σ_y) based on a stochastic model results and we evaluate it by means of the LES results.

2. NUMERICAL SETUP AND SIMULATED CASES

The LES code described by Nieuwstadt and De Valk (1987) is used, in which a conservation equation for the passive tracer is added to the usual set of conservation equations.

An instantaneous line source of scalar is emitted at three different heights ($z_s/z_i = 0.125, 0.25, 0.5$ respectively, where z_s is the release height) after a well mixed

boundary layer has been established. The line source can be equivalently interpreted in terms of a continuous point source. A quasi steady state is reached after a two hours simulation period (initialization) and the diffusion is then investigated during the following hour.

The LES domain covers an area of $10 \times 10 \text{ Km}^2$ solved with a horizontal grid length of 62.5 m. A grid of 40 points is used in the vertical direction; the Boundary Layer (BL) height and the grid resolution changed depending on the case being investigated, on the basis of the different initial conditions (surface heat flux). A time step of 1 s. is used. In order to avoid numerical instabilities the numerical grid (co-ordinate system) translated with the geostrophic wind.

Four different values of the geostrophic wind and three different surface heat fluxes are prescribed and the resulting boundary layers are classified according to the values of the shear-buoyancy ratio u_*/w_* . This ratio plays an important role in the structure of the turbulent field, because it has been shown (e.g. Sykes and Henn (1989), Moeng and Sullivan (1994)) that when this ratio is larger than a critical value (around 0.35) two-dimensional rolls structures tend to form in the velocity fields aligned with the mean wind direction. This change in the turbulent pattern may influence the diffusion process because of the disruption of the horizontal turbulence's isotropy and the increasing of the velocities variances.

In addition to this, the classification proposed by Holtslag and Nieuwstadt (1986) based on the value of the dimensionless height z/z_i and stability parameter z_i/L is used to define three BL archetypes: pure-convection BL ($-z_i/L > 20$), shear-driven BL ($-z_i/L < 10$; near neutral layers) and Shear-Buoyancy (SB) cases in the intermediate regimen where the thermal and mechanical force have the same influence on the generation of turbulence. According to this classification, we expect to find similar dispersion characteristics when the passive tracer is released in one of the boundary layers of the same group. The initial conditions and the dimensionless parameters for the simulated cases are summarized in Table 1.

3. DISPERSION PARAMETERS

After the tracer is released the dispersion's statistics are calculated from the concentration fields computed by the LES model. The (horizontal) dispersion parameter is defined according to Nieuwstadt (1992):

$$\sigma_y^2 = \frac{\int c(y - \bar{y})^2 dV}{\int c dV} \quad (1)$$

* Corresponding author address: A. Dosio, Wageningen University, Meteorology and Air Quality Group, 6701 AP Wageningen, The Netherlands; e-mail: dosio@hp1.met.wau.nl

Cases	$U_g (ms^{-1})$	$-z_i/L$	u_*/w_*	S_*
B1	0.5	7.5×10^4	0.02	0
B2	0.5	1.8×10^3	0.03	0
B3	0.5	5.8×10^3	0.04	0
B4	5	100	0.15	0.17
B5	5	41	0.21	0.27
SB1	5	18	0.27	0.74
SB2	10	10	0.34	0.88
S1	10	4.4	0.45	2.1
S2	15	4.5	0.45	1.6
S3	15	1.9	0.59	3.1

Table 1: Classification of the different simulated cases. The shear term S_* is calculated according to equation (5).

where c is the space-dependent concentration and \bar{y} is the mean plume horizontal position, defined as:

$$\bar{y} = \frac{\int cydV}{\int cdV}. \quad (2)$$

Similar expressions hold for the vertical dispersion parameter σ_z and the velocities variances (σ_v, σ_w).

In a shear-driven BL Venkatram (1988) suggested that the wind shear increases the horizontal dispersion according to:

$$\sigma_y^2 = \sigma_{yb}^2 + \sigma_{ys}^2 \quad (3)$$

where σ_{yb} refers to the buoyancy-generated diffusion and σ_{ys} is the contribution due to the wind shear (shear-generated dispersion). Different expressions have been proposed for the latter which are written below in a general form as:

$$\sigma_{ys}^2 = aS_*^2 f(\sigma_w^b t^c \tau_w^d) \quad (4)$$

where t is time, τ_w is the Lagrangian time for the vertical turbulent velocity and a a constant. The coefficients b , c and d determine the curve's slope ranging from a cubic tendency at small values of t ($b=2, c=3, d=1$) to a linear tendency at large times ($b=-2, c=1, d=-1$). In our study the non dimensional wind direction shear S_* is defined following Luhar (2002) as:

$$S_* = \frac{V}{w_*} \theta_m \quad (5)$$

where θ_m is the wind direction at the mean plume height and V is the total wind intensity ($V^2 = u^2 + v^2$) at the same height.

Explicit testing of expressions (4) are rare by either field campaign or numerical models and therefore our LES results could be useful in deriving and evaluating a suitable parameterization for horizontal dispersion in shear conditions.

4. RESULTS AND DISCUSSION

4.1 Dispersion in a pure-convective BL

Figure 1 shows the dimensionless horizontal dispersion parameter (σ_y/z_i) as function of the non dimensional

turbulent time $t_* \equiv (w_*/z_i)t$ in a pure convective boundary layer. As previously mentioned this comparison is done to verify the model's performance. The results of simulations B1-B5 are averaged and compared with different sets of data.

Our results agree with previous studies, although an exception is found for the recent laboratory data presented by Weil (2002). It has to be noted, however, that a large scatter in the result is present as our boundary layers range from a strong unstable case ($-z_i/L = 5.8 \times 10^3$, $(w'\theta')_0 = 0.156 Wms^{-1}$) to a condition of weaker instability ($-z_i/L = 41$, $(w'\theta')_0 = 0.1 Wms^{-1}$). Weil (2002) suggested that "earlier [laboratory] data are low because of an insufficient detection limit".

The dashed line represents the following expression derived by the Taylor's statistical analysis (arranged from Luhar, 2002):

$$\left(\frac{\sigma_y}{z_i}\right)^2 = 2\left(\frac{\sigma_v}{w_*}\right)^2 \left\{ t_* \tau_* - \tau_*^2 \left(1 - e^{-\frac{t_*}{\tau_*}}\right) \right\} \quad (6)$$

where $\tau_* \equiv \tau_v w_*/z_i$ is the dimensionless lagrangian integral time scale (in the horizontal direction).

Although the theoretical tendency $\sigma_y/z_i \propto t_*^{1/2}$ at large times is well reproduced by all the data series, the slope of the curves depend strongly on the value of the ratio σ_v/w_* . This ratio is usually set equal to 0.6, consistently with the statistical analysis, but lower value were used by Lamb (1982) and Weil (2002). The LES results showed an average value of 0.5.

Moreover, the different contributions of the eddy size to the diffusion process can be analyzed dividing the dispersion parameter in two components: the meandering part (m_y) describing the contribution of the large-scale turbulent eddy motion and the relative dispersions (s_y) related to the increasing size of the plume due to small-scale mixing, as proposed by Nieuwstadt (1992):

$$\sigma_y^2 = m_y^2 + s_y^2 \quad (7)$$

Although Nieuwstadt (1992) already studied the differentiation between meandering and relative diffusion, his results were influenced by the small domain used that limited the horizontal scale of motion. Moreover no data (either field campaign nor laboratory studies) were available at that time for the comparison. An increased domain size and recent available laboratory data (Weil 2002) allow us to investigate the different physical processes governing the plume dispersion and to evaluate in more detail the model results. As it can be seen in figure 1 the contribution of the meandering plays an important role only at short distances ($t_* < 1$) when the plume size is still small and the plume behavior is influenced mainly by the large eddies. The meandering component m_y calculated from the LES agrees well with the laboratory data and approaches a constant value as prescribed by theoretical studies (Weil, 2002).

4.2 Dispersion in a shear-driven BL

Figure 2 shows the horizontal dispersion parameter calculated from the LES concentration fields in the differ-

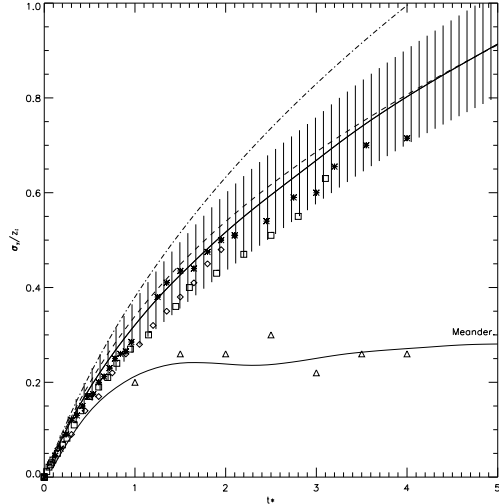


FIG. 1: Horizontal dispersion parameter for the pure-buoyancy cases: Solid line: LES results averaged over the pure-buoyancy cases (Vertical bars are the standard deviations); Stars; Willis and Deardorff (1981); Squares: Lamb (1982); Diamonds: Nieuwstadt and De Valk (1987); Dot-dashed line: Weil (2002); Dashed line: parameterization (eq 6). In the same picture the meandering component is shown and the data from Weil (2002) are compared (triangles).

ent shear-driven BL (solid lines). The pure buoyancy case (B1-B5) is shown for comparison. Cases SB1 and SB2 have values of the shear-buoyancy ratio u_*/w_* around 0.3. As discussed previously, in these conditions the turbulent pattern is changed and the horizontal isotropy is disrupted by the formation of two-dimensional rolls. This results in an increase of the plume spreading as shown in the figure.

For larger values of the wind shear (cases S1, S2 and S3) the dispersion parameter can reach at large times a value that is as twice as large than in the pure buoyancy cases, in agreement with previous studies (Mason, 1993).

As stated previously, the different contributions of the buoyancy and the shear can be analyzed by dividing the total dispersion parameter in a buoyancy-generated diffusion σ_{yb} and a shear contribution σ_{ys} (shear-generated dispersion), according to equation (3). In our study the buoyancy-generated dispersion is parameterized with equation (6) and the shear contribution is described according to Luhar (2002) as follows:

$$\sigma_{ys}^2 = \frac{a_0 S_*^2 \sigma_w^2 \tau_w t_*^2 z_i / w_*}{\left[1 + \left(\frac{t}{t_0}\right)^3\right]^{2/3}} \quad (8)$$

Equation (8) is an interpolation between the t^3 and linear dependence discussed previously in equation (4). The time t_0 marks the transition between the two tendencies and it is defined as:

$$t_0 = \left(\frac{z_i^4}{a_0 b_0 \sigma_w^4 \tau_w \tau_c}\right)^{(1/2)} \quad (9)$$

The value of the constants a_0 and b_0 are fixed to 0.09 and 60 respectively, and $\tau_c = 0.9z_i/w_*$.

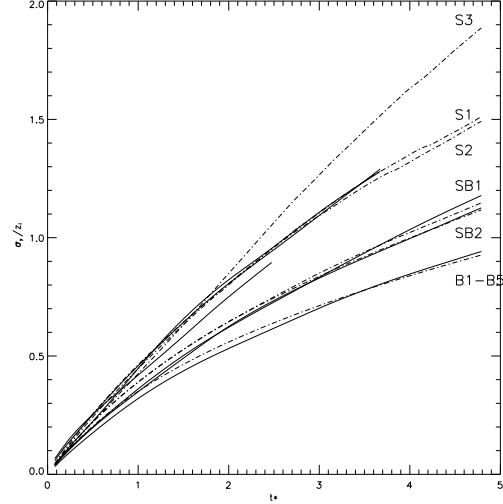


FIG. 2: Horizontal dispersion parameter for the pure-buoyancy and shear cases: Solid line: LES results (the pure-buoyancy cases B1-B5 have been averaged as explained before); Dashed-dotted line: parameterization (equation 3).

As shown in figure 2 the parameterization (dashed-dotted lines) agrees satisfactorily when compared with the model results. The LES results for the SB1 and SB2 cases are very similar: notice that in Table 1 these two cases have similar stability parameters and similar values for the shear. Therefore similar dispersion characteristics are expected and the LES results confirm this hypothesis.

Cases S1 and S2 also have the same values of the shear-buoyancy ratio u_*/w_* and the stability parameter $-z_i/L$. The LES results give very similar results for these cases, in agreement with the above mentioned classification. It is worthwhile noting, on the other hand, that the values of the wind shear in the two cases are different ($S_* = 2.1$ and $S_* = 1.6$). As the shear-generated dispersion at large times is proportional to the wind shear (equation 4) one can expect that the shear contribution in case S1 is larger than in case S2. On the other hand, the buoyancy-generated dispersion σ_{yb} is proportional to the horizontal velocity variance (equation 6) and Sykes and Henn (1989) showed that an increase in the geostrophic wind (U_g in case S2 is larger than in case S1, see Table 1) enhances the value of the velocity variances so that the value of σ_{yb} is larger in case S2 than in case S1. When the two contributions are added according to equation (3) the resulting total dispersion parameter in the two cases therefore has a similar value.

The dimensionless shear-generated dispersion parameter σ_{ys}/z_i is shown in figure 3. The shear contribution is comparable to the buoyancy-generated dispersion σ_{yb} for values of the shear around 2.1 (case S1) a result that is consistent with the analysis of Luhar (2002). Our results for cases S1 S2 and S3 show that when the

mechanical forcing becomes comparable to the thermal forcing ($u_*/w_* > 0.3$), the wind shear influences the dispersion process even at short times ($t_* < 2$). This is often neglected by the parameterizations used in the applied dispersion models.

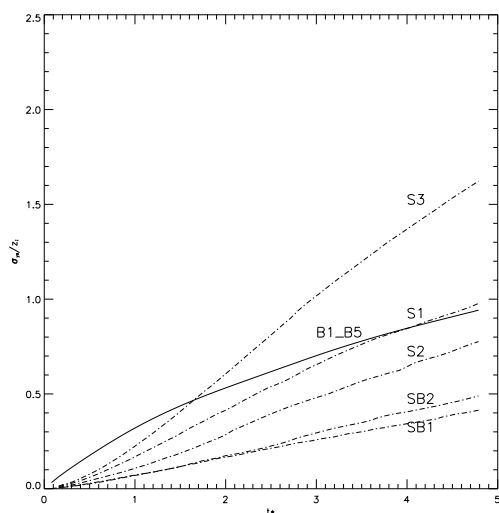


FIG. 3: Shear-generated dispersion; for comparison the buoyancy-generated dispersion (Cases B1-B5; no shear) is reported as solid line.

5. CONCLUSIONS

Wind shear is an important factor in the dispersion of an inert tracer in a Convective Boundary Layer because it enhances the horizontal plume spread. To evaluate this impact, the dispersion of a line source of passive tracer emitted in a CBL was studied by means of a Large Eddy Simulation. Several idealized Boundary Layers were generated with different combinations of thermal and mechanical forcing and classified according to stability parameters. The model results for the pure buoyancy cases were compared with different series of data showing good agreement with laboratory observations, numerical simulations and theoretical expressions. The comparison was extended to validate the meandering and relative dispersion contributions. The LES results confirmed recent laboratory data and showed that meandering is an important factor for $t_* < 1$. Dispersion in shear-driven boundary layers was also studied and the effect of the wind shear analyzed. The total dispersion parameter σ_y was divided into two contributions: the buoyancy-generated dispersion σ_{yb} and the shear contribution σ_{ys} related to the wind shear. A parameterization was compared to the LES data with satisfactory results. The shear contribution σ_{ys} became relevant when the shear-buoyancy ratio u_*/w_* approached a value around 0.3. For larger values of the wind shear (S_*) the shear-generated dispersion became comparable to the buoyancy-generated dispersion. Future work will investigate the effect of shear on ground

concentrations and concentration fluctuations. The analysis of the differentiation between meandering and relative diffusion in shear-driven BL will be also analyzed.

References

- Gryning, S. E. et al., 1987: Applied Dispersion modelling based on meteorological scaling parameters, *Atm. Env.*, **21**, 79-89.
- Holtslag A. A. M and F. T. M. Nieuwstadt, 1986: Scaling the atmospheric boundary layer. *Boundary-Layer Met* **36**, 201-209.
- Lamb, R. G., 1982: Diffusion in the convective boundary layer; in F. T. M. Nieuwstadt and H. van Dop (eds.) *Atmospheric Turbulence and Air Pollution Modelling*, Reidel Publishing Company, Dordrecht, pp. 159-229.
- Luhar, A. K., 2002: The influence of vertical wind direction shear on dispersion in the convective boundary layer and its incorporation in coastal fumigation models. *Bound.-Layer Meteor.* **102**, 1-38.
- Mason, P. J., 1992: Large Eddy simulation of dispersion in convective boundary layer with wind shear, *Atm. env.*, **26A**, 1561-1571.
- Moeng, C.-H. and P. P. Sullivan, 1994: A comparison of shear- and buoyancy-driven planetary boundary layer flows, *J. Atm. Sc.*, **7**, 999-1022.
- Nieuwstadt F. T. M. and J. P. J. M. M. de Valk, 1987: A Large eddy simulation of buoyant and non-buoyant plume dispersion in the atmospheric boundary layer. *Atm. env.* **21**, 2573-2587.
- Nieuwstadt, F. T. M., 1992: A Large Eddy simulation of a line source in a convective atmospheric boundary layer-I. dispersion characteristics, *Atm. Env.*, **26A**, 485-495.
- Sykes, R. I. and D. S. Henn, 1989: Large Eddy Simulation of turbulent sheared convection, *J. Atm. Sc.*, **46**, 1106-1118.
- Venkatram, A., 1988: Dispersion in the Stable Boundary Layer; in A.Venkatram and C.J.Wyngaard (eds.), *Lectures on Air Pollution Modelling*, American Meteorological Society, Boston, MA, pp. 229-265.
- Weil, J. C., 2002: Experiments on buoyant plume dispersion in a laboratory convection tank. *Bound.-Layer Meteor.* **102**, 367-414.
- Willis, G. E. and J. W. Deardorff, 1981: A laboratory study of dispersion from a source in the middle of the convectively mixed layer, *Atm. Env.*, **15**, 109-117.